Gamow-Teller and double-beta decays of heavy nuclei within an effective theory

E. A. Coello Pérez,[1,2] J. Menéndez,[3] and A. Schwenk[1,2,4]

[1] Institut für Kernphysik, Technische Universität Darmstadt, 64289 Darmstadt, Germany
[2] ExtreMe Matter Institute EMMI, Helmholtzzentrum für Schwerionenforschung GmbH, 64291 Darmstadt, Germany
[3] Center for Nuclear Study, The University of Tokyo, Tokyo 113-0033, Japan
[4] Max-Planck-Institut für Kernphysik, Saupfercheckweg 1, 69117 Heidelberg, Germany

We study β decays within an effective theory that treats nuclei as a spherical collective core with an even number of neutrons and protons that can couple to an additional neutron and/or proton. First we explore Gamow-Teller β decays of parent odd-odd nuclei into low-lying ground, one-phonon, and two-phonon states of the daughter even-even system. The low-energy constants of the effective theory are adjusted to data on β decays to ground states or Gamow-Teller strengths. The corresponding theoretical uncertainty is estimated based on the power counting of the effective theory. For a variety of medium-mass and heavy isotopes the theoretical matrix elements are in good agreement with experimental results within the theoretical uncertainties. We then study the two-neutrino double-β decay into ground and excited states. The results are remarkably consistent with experiment within theoretical uncertainties, without the necessity to adjust any low-energy constants.

I. INTRODUCTION

Atomic nuclei are sensitive to fundamental interactions beyond the strong force that binds them. Excited states typically decay due to electromagnetic interactions emitting γ rays, while unstable nuclear ground states decay via weak interactions emitting or capturing electrons, neutrinos, or their antiparticles. Nuclei are also used as laboratories due to their sensitivity to new-physics interactions beyond the Standard Model [1–3].

The weak interaction is closely connected to ground-state decays. Almost every unstable isotope lighter than ^{208}Pb decays either via β decay or electron capture. The associated half-lives can range from milliseconds to billions of years, with the corresponding nuclear transition matrix elements varying by three or more orders of magnitude. This wide range makes theoretical predictions of β decay and electron capture particularly challenging tests of nuclear-structure calculations. Reliable predictions are also especially important for astrophysics because β-decay half-lives of experimentally inaccessible very neutron-rich nuclei set the scale of the rapid-neutron capture, or r-process, which is responsible for the nucleosynthesis of heavy elements [4–6].

Ab initio calculations of β decays are still limited to few-nucleon systems (see, e.g., Refs. [7–9]) or focus on selected lighter isotopes [10, 11]. For medium-mass and heavy nuclei theoretical studies typically use the quasiparticle random-phase approximation (QRPA) (see, e.g., Refs. [12–18]), sometimes combined with more macroscopic calculations [19], and when possible the nuclear shell model (see, e.g., Refs. [20–23]). The agreement of these many-body calculations with experimental data demands fitting part of the nuclear interactions and/or the effective operators, such as the isoscalar pairing for the QRPA or a renormalization ("quenching") factor for the transition operator in shell model calculations [24, 25]. At present, the predictions made by different methods for non-measured decays disagree by factors of a few units. Furthermore, in these phenomenological calculations it is difficult to provide well founded estimates of the associated theoretical uncertainties.

Second-order processes in the weak interaction, double-β ($\beta\beta$) decays, have been observed in otherwise stable nuclei. They exhibit the longest half-lives measured to date, exceeding 10^{19} years [26]. This decay mode is via two-neutrino $\beta\beta$ ($2\nu\beta\beta$) decay, to distinguish it from an even more rare type of $\beta\beta$ decay without neutrino emission, neutrinoless $\beta\beta$ ($0\nu\beta\beta$) decay, which is so far unobserved. The latter process is not allowed by the Standard Model since it violates lepton number conservation, and can only occur if neutrinos are their own antiparticles. $0\nu\beta\beta$ decay is the object of very intense experimental searches [27–30] with the goal of elucidating the nature of neutrinos. The calculation of matrix elements for $\beta\beta$ decays is specially subtle [31–34]. It faces challenges similar to those of β decays, with the additional difficulty that $\beta\beta$ decays are suppressed. As with β decays, calculations by different many-body approaches of unknown nuclear matrix elements vary by factors of a few units. The prediction of reliable matrix elements with theoretical uncertainties is especially pressing for the interpretation and planning of present and future $0\nu\beta\beta$ decay experiments.

The goal of this work is to use an effective theory (ET) framework to study the β, electron capture, and $\beta\beta$ decays of medium-mass and heavy nuclei. Calculations within an ET can provide transition matrix elements with quantified theoretical uncertainties, and are therefore a good complement to existing many-body β-decay studies. We focus on Gamow-Teller (GT) transitions for which experimental data are available, leaving the study of $0\nu\beta\beta$ decay for future work. The ET used here is valid for transitions involving spherical systems, because nuclei are treated as a spherical collective core coupled to a few nucleons.

Over the past decades, ETs have been applied to describe the low-energy properties of nuclei. Effective theories exploit the separation of scales between the low-energy physics governing the processes of interest, which are treated explicitly, and the high-energy physics whose effects are integrated out and encoded into low-energy constants (LECs) that must be fit to experimental data. The ET is formulated in terms of the low-energy degrees of freedom (DOF) and their interactions, consistent with the symmetries of the underlying theory. The ET offers a systematic order-by-order expansion based on a power counting given by the ratio of the low-energy over the breakdown scale, at which the ET is no longer valid. This also allows for the quantification of the theoretical uncertainties at a given order in the ET [35–38].

Effective field theories have been very successful in describing two- and three-nucleon forces in terms of nucleon and pion fields [39–43]. In combination with powerful *ab initio* methods, chiral interactions have been employed to calculate low-energy properties of light and medium-mass isotopes (see, e.g., recent reviews [44–48]). Complementary, a different set of ETs has been proposed to describe heavy nuclei in terms of collective DOF [49–55]. In particular, the ET developed in Refs. [54, 55] describes the low-energy properties of spherical even-even and odd-mass nuclei in terms of effective single-particle DOF coupled to a collective spherical core. Using this approach, the low-energy spectra and electromagnetic properties of even-even and odd-mass nuclei (the latter with $1/2^-$ ground states) were described consistently, in good agreement with experiment [55]. The electromagnetic strength between low-lying states, including magnetic dipole transitions in odd-mass systems, was predicted successfully. Since for β decays the relevant physics is expected to be like that of magnetic dipole transitions, the ET framework offers a promising approach to describe β, electron capture, and $\beta\beta$ decays in nuclei.

This paper is organized as follows. Section II serves as a short summary of key elements from the theory of β, electron capture and $\beta\beta$ decays. Section III begins with a brief introduction to the ET of spherical even-even nuclei followed by an extension of the theory to account for the low-lying states of odd-odd nuclei. Next we discuss the GT transition operator that enters β decays as well as methods to fix the associated LECs. In Sec. IV we present our ET results for β decay matrix elements of spherical odd-odd nuclei with $1^+_{\rm gs}$ ground states into final states of even-even nuclei corresponding to different collective ET excitations. We compare the ET predictions with experimental data, including the estimated theoretical uncertainties. In Sec. V we test the ability of the ET to consistently describe β and $2\nu\beta\beta$ decays, without the necessity to adjust additional LECs. We conclude with a brief summary and outlook in Sec. VI.

II. TYPES OF β DECAYS

A. Single-β decay and electron capture

The most common weak interaction process is β decay. Here either one of the N neutrons in a nucleus decays into a proton (β^- decay), or one of the Z protons decays into a neutron (β^+ decay). The total number of nucleons A remains the same. For the electric charge, lepton number, and angular momentum to be conserved, it is required that an electron (e^-) or positron (e^+) be emitted along with an electron antineutrino ($\overline{\nu}_e$) or neutrino (ν_e):

$$A(Z,N) \xrightarrow{\beta^-} A(Z+1,N-1) + e^- + \overline{\nu}_e\,, \qquad (1)$$

$$A(Z,N) \xrightarrow{\beta^+} A(Z-1,N+1) + e^+ + \nu_e\,. \qquad (2)$$

Alternatively, proton-rich nuclei can undergo a third process, an electron capture (EC), which involves the capture of an electron by a proton, yielding a neutron. Again, conservation of energy, angular momentum, and lepton number requires an electron neutrino to be emitted:

$$A(Z,N) + e^- \xrightarrow{\rm EC} A(Z-1,N+1) + \nu_e\,. \qquad (3)$$

At lowest order in the weak interaction, it is possible to distinguish two types of dominant, so-called allowed, transitions. Gamow Teller and Fermi (F) decays differ in the spin dependence of the associated one-body operator. The GT and F operators are defined as

$$O_{\rm GT} = \sum_{a=1}^{A} \boldsymbol{\sigma}_a \tau_a^{\pm}\,, \qquad (4)$$

$$O_{\rm F} = \sum_{a=1}^{A} \tau_a^{\pm}\,, \qquad (5)$$

where $\boldsymbol{\sigma}$ denotes the spin, τ^+ (τ^-) is the isospin raising (lowering) operator, and a sum is performed over all nucleons in the nucleus.

In this work, we focus on allowed GT transitions, whose decay rates are related to the reduced matrix elements of the GT operator in Eq. (4) between the corresponding initial (i) and final (f) nuclear states:

$$M_{\rm GT} = \langle f||O_{\rm GT}||i\rangle\,. \qquad (6)$$

The decay's half-life is given by

$$\frac{1}{t_{if}} = \frac{f_{if}}{\kappa}\frac{g_A^2\,|M_{\rm GT}|^2}{2J_i+1}\,, \quad \text{or} \quad (ft)_{if} = \frac{\kappa}{g_A^2}\frac{2J_i+1}{|M_{\rm GT}|^2}\,. \qquad (7)$$

Here the phase-space factor f_{if} contains all the information on the lepton kinematics, $\kappa = 6147$ s is the β-decay constant, $g_A = 1.27$ is the axial-vector coupling, and J_i denotes the total angular momentum of the initial state. The quantity $(ft)_{if} \equiv f_{if}t_{if}$ is known as the ft-value and is directly comparable to the transition nuclear matrix element.

B. $2\nu\beta\beta$ decays

In the $2\nu\beta\beta$ decay, two neutrons of the parent even-even nucleus decay into two protons. Two electrons and antineutrinos are emitted as well due to charge and lepton-number conservation:

$$A(Z,N) \xrightarrow{2\beta^-} A(Z+2,N-2) + 2e^- + 2\overline{\nu}_e\,. \tag{8}$$

Such decays have been detected for several nuclei, including a few cases of transitions into excited states [26]. At present the similar but kinematically less favored $\beta^+\beta^+$ and the 2ν double-electron-capture (ECEC) decays have only been observed in geochemical measurements for ^{130}Ba [56, 57], and there is also an indication of a possible detection in ^{78}Kr [58].

In principle, both GT and F operators enter the description of $2\nu\beta\beta$ decays. Nevertheless, in decays to low-lying states of the final daughter nucleus only the GT part is relevant. The F operator does not connect states with different isospin quantum numbers, and its strength is almost completely exhausted by the isobaric analog state, which lies at an excitation energy of tens of MeVs. The decay rate for $2\nu\beta\beta$ decay is then [34]

$$\frac{1}{t_{if}^{2\nu\beta\beta}} = G_{if}^{2\nu\beta\beta} g_A^4 \left| M_{\rm GT}^{2\nu\beta\beta} \right|^2 , \tag{9}$$

where $G_{if}^{2\nu\beta\beta}$ is a phase-space factor, and the nuclear matrix element $M_{\rm GT}^{2\nu\beta\beta}$ is given by

$$M_{\rm GT}^{2\nu\beta\beta} = \sqrt{\frac{1}{s}} \sum_n \frac{\langle f || \sum_a \boldsymbol{\sigma}_a \tau_a^+ || 1_n^+ \rangle \langle 1_n^+ || \sum_b \boldsymbol{\sigma}_b \tau_b^+ || i \rangle}{(D_{nf}/m_e)^s} , \tag{10}$$

where the electron mass m_e is introduced to make the matrix element dimensionless, $s \equiv 1 + 2\delta_{2J_f}$ with $J_f = 0, 2$ being the spin of the final state, and the sum runs over all $|1_n^+\rangle$ states of the intermediate odd-odd nucleus. The energy denominators D_{nf} are given in terms of the energy of the initial (i), final (f), and intermediate (n) states by

$$D_{nf} = E_n - \frac{E_i - E_f}{2} \,. \tag{11}$$

III. ET FOR SINGLE-β DECAY

In this section, we formulate an ET for the GT decays of parent odd-odd into daughter even-even nuclei. Our approach is valid for spherical systems with low-energy spectra and electromagnetic transitions well reproduced by an ET written in terms of collective DOF, which at leading order (LO) represent a five-dimensional harmonic oscillator. The ET DOF are therefore similar to those in the collective Hamiltonian of Bohr and Mottelson [59–62] or the interacting boson model [63–68]. An advantage is that in the ET the theoretical uncertainties due to omitted DOF can be propagated to the nuclear matrix elements and decay half-lives, allowing for a more informed comparison of the ET predictions with experimental data.

A. ET for even-even and odd-odd nuclei

The ET developed in Refs. [54, 55] describes the low-energy properties of spherical even-even and odd-mass nuclei in terms of collective excitations that can be coupled to an odd neutron, neutron-hole, proton, or proton-hole. The effective operators are written in terms of creation and annihilation operators, which are the DOF of the ET. These include the following:

i) Collective phonon operators $d_\mu^\dagger$ and d_μ, which create and annihilate quadrupole phonons associated with low-energy quadrupole excitations of the even-even core.

ii) Neutron operators $n_\mu^\dagger$ and n_μ, which create and annihilate a neutron or neutron-hole in a $j_n^{\pi_n}$ single-particle orbital with total angular momentum j and parity π.

iii) Proton operators $p_\mu^\dagger$ and p_μ, which create and annihilate a proton or proton-hole in a $j_p^{\pi_p}$ orbital.

Whether the fermion operators represent a particle or a hole depends on the odd-mass nucleus we want to describe and the even-even nucleus chosen as a core. In Ref. [55], silver isotopes with $1/2^-$ ground states were described both as an odd proton coupled to palladium cores and as an odd proton-hole coupled to cadmium cores. Both descriptions turned out to be consistent with each other. The above operators fulfill the following relations

$$\left[d_\mu, d_\nu^\dagger\right] = \delta_{\mu\nu}\,, \quad \left\{n_\mu, n_\nu^\dagger\right\} = \delta_{\mu\nu}\,, \quad \left\{p_\mu, p_\nu^\dagger\right\} = \delta_{\mu\nu}\,. \tag{12}$$

While the creation operators are the components of spherical tensors, the annihilation operators are not. To facilitate the construction of spherical-tensor operators with definite ranks, we define annihilation spherical tensors with components $\tilde{a}_\mu = (-1)^{j_a+\mu} a_{-\mu}$, where $a = d, n, p$ and $j_d = 2$.

The Hamiltonian employed in previous work to describe the energy spectra of a particular even-even nucleus and an adjacent odd-mass nucleus at next-to-leading order (NLO) is

$$H_{\rm ET}^{\rm NLO} = \omega \left(d^\dagger \cdot \tilde{d}\right) + \sum_{fl} g_{fl} \left(d^\dagger \otimes \tilde{d}\right)^{(l)} \cdot \left(f^\dagger \otimes \tilde{f}\right)^{(l)} , \tag{13}$$

where f can be either n or p, depending in which odd-mass nucleus we want to describe, and ω and g_{fl} are LECs that must be fitted to data. The LEC accompanying the LO term, ω, may be thought of as the energy of the collective mode. It scales as the excitation energy of the first excited 2^+ state of the even-even nucleus of interest. Terms proportional to g_{fl} are required to describe the spectrum of the odd-mass nucleus at NLO. The energy scale Λ at which the ET breaks down lies around the three-phonon level. Based on previous work [54], we will set $\Lambda = 3\omega$ in what follows, even though the breakdown scale might not be exactly the same for every pair of nuclei studied in this work. The effective operators of the theory are constructed order-by-order adding all relevant terms that correct the previous one by a positive power of $\varepsilon \equiv \omega/\Lambda$.

The reference state $|0\rangle$ of the ET represents the $0^+_{\rm gs}$ ground state of the even-even nucleus of interest. Multi-phonon excitations of this state represent excited states in the even-even system. Of particular relevance for our work are one- and two-phonon excitations:

$$|2M1\rangle = d^\dagger_M|0\rangle\,, \quad \text{and} \quad |JM2\rangle = \sqrt{\frac{1}{2}}\left(d^\dagger \otimes d^\dagger\right)^{(J)}_M|0\rangle\,, \tag{14}$$

where in the notation $|JM\mathcal{N}\rangle$, J and M are the total angular momenta of the state and its projection, and $\mathcal{N}$ is the number of phonons. We define the coupling of two spherical tensors as in Ref [69], and refer to Ref. [62] for a detailed description of the construction of multi-phonon excitations. We highlight that the ET introduced above reproduces the low-lying spectra and electromagnetic moments and transitions of vibrational medium-mass and heavy nuclei within the estimated theoretical uncertainties [54].

In a similar fashion, the ground states of adjacent odd-mass nuclei can be described as fermion excitations of the reference state

$$|j_f M\rangle = f^\dagger_M|0\rangle\,, \tag{15}$$

while excited states in these systems are represented by their multiphonon excitations. Even though several single-particle orbitals may be relevant to give a full description of the odd-mass states, it is assumed that at LO in the ET only one orbital is required to describe the low-energy properties of these systems. The relevant single-particle orbital is inferred from the quantum numbers of the ground state of the odd-mass nucleus of interest. This assumption works well for odd-mass nuclei near shell closures with $1/2^-$ ground states [55]. In these systems, a reasonable agreement was found between the ET predictions and experimental data, regarding not only low-energy excitations but also electric and magnetic moments and transitions [55].

In order to describe the allowed GT β decays of parent odd-odd nuclei, we extend the collective ET of Refs. [54, 55] and write the low-lying positive-parity states in the odd-odd nucleus as

$$|JM;j_p;j_n\rangle = \left(n^\dagger \otimes p^\dagger\right)^{(J)}_M|0\rangle\,, \tag{16}$$

where the fermion operators represent particles or holes depending on the odd-odd nucleus of interest. For example, ^{80}Br can be described coupling a neutron and a proton hole to a ^{80}Kr core, or coupling a neutron hole and a proton to a ^{80}Se core. The j_n and j_p labels in the odd-odd state indicate the coupling of the odd neutron and odd proton on top of the collective spherical ground state. The angular momentum and parity of the single-particle orbitals to be used are inferred from the quantum numbers of the low-lying states of the adjacent odd-mass nuclei. Therefore, the total angular momenta and parities of these orbitals must fulfill the relations $|j_n - j_p| \leqslant J \leqslant j_n + j_p$, and $\pi_n\pi_p = 1$ for positive-parity states. The correction

$$\Delta H^{\rm NLO}_{\rm ET} = \sum_l \epsilon_l \left(n^\dagger \otimes \tilde{n}\right)^{(l)} \cdot \left(p^\dagger \otimes \tilde{p}\right)^{(l)}\,, \tag{17}$$

must be added to the Hamiltonian in Eq. (13) in order to account for the mass difference between the even-even and odd-odd ground states. It is important to note that the LO calculation of single-β decays of the ground states of odd-odd nuclei require us to construct their energy spectra only at LO, simplifying the calculations considerably as the terms proportional to g_{fl} in Eq. (13) do not enter at this order. Contributions due to additional DOF relevant for excited states are taken into account in the uncertainty estimates associated with the LO results. We stress that these uncertainties must be tested whenever data are available, since they probe the validity of the power counting and the reliability of the LO calculations.

B. Effective GT operator

Next we construct the operator corresponding to the GT operator in Eq. (4), in terms of the effective DOF. We write the most general positive-parity spherical-tensor operator of rank one capable of coupling the low-lying states of the parent odd-odd nucleus introduced in Eq. (16) to the ground, one-phonon, and two-phonon states of the daughter even-even nucleus represented in Eq. (14). At lowest order in the number of d operators, this operator is given by

$$\begin{aligned} O_{\rm GT} = &\, C_\beta \left(\tilde{p} \otimes \tilde{n}\right)^{(1)} \\ &+ \sum_\ell C_{\beta\ell}\left[\left(d^\dagger + \tilde{d}\right) \otimes \left(\tilde{p} \otimes \tilde{n}\right)^{(\ell)}\right]^{(1)} \\ &+ \sum_{L\ell} C_{\beta L\ell}\left[\left(d^\dagger \otimes d^\dagger + \tilde{d} \otimes \tilde{d}\right)^{(L)} \otimes \left(\tilde{p} \otimes \tilde{n}\right)^{(\ell)}\right]^{(1)}\,, \end{aligned} \tag{18}$$

where C_β, $C_{\beta\ell}$, and $C_{\beta L\ell}$ are LECs that must be fit to experimental data.

Let us discuss the effective operator of Eq. (18) in more detail. For the allowed GT β^- decay of the odd-odd nucleus with $N+1$ neutrons and $Z-1$ protons into the even-even nucleus with N neutrons and Z protons, the odd-odd system is described within the ET as an even-even core coupled to a neutron and a proton hole. For the decay to take place, the fermion annihilation operators must annihilate the odd neutron and proton hole. This action represents the decay of a neutron in the odd-odd system into a proton, which then fills the proton hole, yielding the even-even system. An additional step in which the odd neutron fills a neutron hole takes place if the annihilated neutron is part of the core; however, the ET cannot differentiate between the two processes. For the description of the β^+ or EC decay to the even-even nucleus with $N+2$ neutrons and $Z-2$ protons, it is more convenient to describe the odd-odd nucleus in terms of the later $(N+2, Z-2)$ even-even core coupled to a neutron hole and a proton. In this case, the fermion annihilation operators annihilate the odd neutron hole and proton, representing the conversion of a proton into a neutron that fills the neutron hole. Again, the additional filling of a proton hole by the odd proton follows if the annihilated proton is in the core.

The reduced matrix elements of the effective GT operator in Eq. (18) between low-lying states of the parent odd-odd system in Eq. (16) and the daughter even-even ground, one-phonon, and two-phonon states in Eq. (14) are

$$M_{\rm GT}\left(J_i^+ \to 0_{\rm gs}^+\right) = \begin{cases} -C_\beta\sqrt{3}(-1)^{j_p-j_n+J_i} & J_i = 1 \\ 0 & \text{otherwise} \end{cases}, \tag{19}$$

$$M_{\rm GT}\left(J_i^+ \to 2_{\rm 1ph}^+\right) = \begin{cases} C_{\beta J_i}\sqrt{3}(-1)^{j_p-j_n+J_i} & |J_i-1| \leqslant 2 \leqslant J_i+1 \\ 0 & \text{otherwise} \end{cases}, \tag{20}$$

$$M_{\rm GT}\left(J_i^+ \to J_{\rm 2ph}^+\right) = \begin{cases} C_{\beta J_{\rm 2ph} J_i}\sqrt{6}(-1)^{j_p-j_n+J_i} & |J_i-1| \leqslant J_{\rm 2ph} \leqslant J_i+1 \\ 0 & \text{otherwise} \end{cases}, \tag{21}$$

where the subscripts gs and $n$ph identify the ground and n-phonon states of the daughter even-even nucleus, respectively. We also note that the LECs in Eqs. (19)–(21) implicitly take into account additional corrections to the GT operator in Eq. (4), such as a possible "quenching".

C. ET GT decay to ground and excited states

The first, second, and third terms of the effective GT operator in Eq. (18) couple states with phonon-number differences of zero, one, and two, respectively. Thus, they describe the β decays from the ground state of the odd-odd nucleus to the ground, one-phonon, and two-phonon states in the even-even nucleus, respectively. Figure 1 schematically shows the case of the β decays of ^{80}Br into the $0^+_{\rm gs}$, 2^+_1, 2^+_2 and 0^+_2 states of ^{80}Kr, identified as the ground, one-phonon, and two-phonon states.

The LECs C_β, $C_{\beta J_i}$, and $C_{\beta J_{\rm 2ph} J_i}$ encode the microscopic information of the nuclei involved in the decay. While the value of the LECs is not predicted by the ET, the power counting established in previous works [54, 55] suggests scaling factors between them. This power counting is based on the assumption that at the energy scale Λ where the ET breaks down, the matrix elements of every term of any effective operator scale similarly.

From this assumption and the effective Hamiltonian describing the even-even systems, it can be concluded that at the breakdown scale Λ the matrix elements of an operator containing n powers of d operators scale as [54]

$$\langle d^n \rangle \sim \left(\frac{\Lambda}{\omega}\right)^{n/2}. \tag{22}$$

For more details, we refer the reader to Ref. [54].

The power counting in Eq. (22) implies that at the

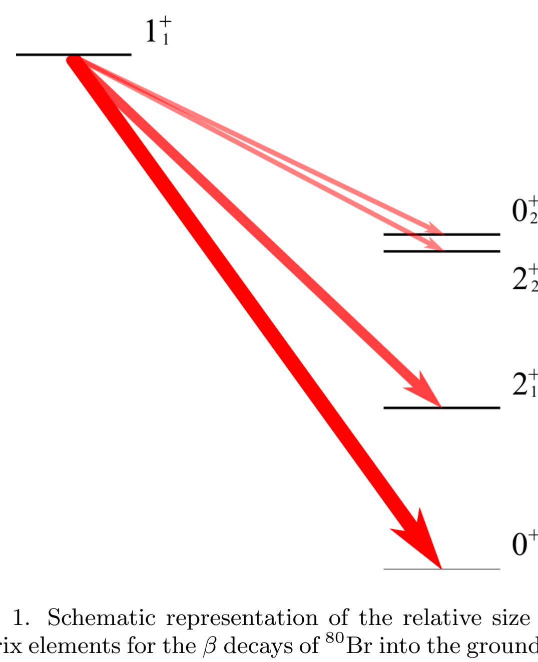

FIG. 1. Schematic representation of the relative size of the matrix elements for the β decays of ^{80}Br into the ground ($0^+_{\rm gs}$), one-phonon (2^+_1), and two-phonon (0^+_2, 2^+_2) excited states of ^{80}Kr.

breakdown scale Λ the matrix elements of the different terms in the effective GT operator (18) scale as

$$C_\beta \langle d^0 \rangle \sim C_{\beta J_i} \langle d^1 \rangle \quad \text{or} \quad \frac{C_{\beta J_i}}{C_\beta} \approx 0.58(^{+42}_{-25})\,, \tag{23}$$

and

$$C_\beta \langle d^0 \rangle \sim C_{\beta J_{2\mathrm{ph}} J_i} \langle d^2 \rangle \quad \text{or} \quad \frac{C_{\beta J_{2\mathrm{ph}} J_i}}{C_\beta} \approx 0.33(^{+25}_{-14})\,. \tag{24}$$

The resulting relative sizes of the matrix elements for the ^{80}Br decay are also shown schematically in Fig. 1. The theoretical uncertainties for the above ratios have been estimated based on the expectation for the next-order LECs C to be of natural size, encoded into prior distributions of the form

$$\mathrm{pr}(C|c) = \frac{1}{\sqrt{2\pi} c} e^{-\frac{1}{2}\left(\frac{C-1}{c}\right)^2}\,, \tag{25}$$

$$\mathrm{pr}(c) = \frac{1}{\sqrt{2\pi}\sigma c} e^{-\frac{1}{2}\left(\frac{\log c}{\sigma}\right)^2}\,, \tag{26}$$

with $\sigma = \log(3/2)$, so that a value for a LEC in the range $\sqrt{\omega/\Lambda} \leq C \leq \sqrt{\Lambda/\omega}$ with $\Lambda = 3\omega$ has an associated theoretical uncertainty given by an interval of its probability distribution function with a 68% degree of belief. Finally, we emphasize that these theoretical uncertainty estimates must be tested by comparing the ET predictions to data.

D. ET GT decay to ground states and theoretical uncertainties

The matrix elements of single-β decays to the ground state are set by the values of the LEC C_β, see Eq. (18), which are to be fitted to experimental data. Within the ET the uncertainty of these matrix elements comes from two sources:

i) Omitted terms in the effective GT operator that involve two d operators and couple states of odd-odd and even-even nuclei with the same number of phonons. The matrix elements of these terms are expected to scale as

$$\langle 0^+_{\mathrm{gs}} | \Delta O_{\mathrm{GT}} | J_i^+ \rangle \sim \frac{\omega}{\Lambda} M_{\mathrm{GT}} \left(J_i^+ \to 0^+_{\mathrm{gs}} \right). \tag{27}$$

ii) Next-to-leading-order corrections to the ground state of odd-odd nuclei due to terms in the Hamiltonian that can mix states with phonon-number differences of one. These corrections are expected to scale as $\sqrt{\omega/\Lambda}|JM; j_p; j_n\rangle$ and are coupled to the even-even ground state by the second term of the effective GT operator, which contains an additional d operator. Therefore, the corrections to the matrix elements also scale as

$$\langle 0^+_{\mathrm{gs}} | O_{\mathrm{GT}} \Delta | J_i^+ \rangle \sim \frac{\omega}{\Lambda} M_{\mathrm{GT}} \left(J_i^+ \to 0^+_{\mathrm{gs}} \right). \tag{28}$$

From here, the uncertainty estimate associated to the matrix element in Eq. (19) is

$$\Delta M_{\mathrm{GT}} \left(J_i^+ \to 0^+_{\mathrm{gs}} \right) \sim \frac{\omega}{\Lambda} M_{\mathrm{GT}} \left(J_i^+ \to 0^+_{\mathrm{gs}} \right). \tag{29}$$

Consequently, the uncertainty associated to the $\log(ft)$ of the decay to the ground state is estimated as the next-order contribution to the Taylor expansion of the logarithm of the argument in Eq. (7) with $M_{\mathrm{GT}} \left(J_i^+ \to 0^+_{\mathrm{gs}} \right) \approx (1 \pm \omega/\Lambda) M_{\mathrm{GT}} \left(J_i^+ \to 0^+_{\mathrm{gs}} \right)$, that is,

$$\Delta \log(ft)_{if} \sim \frac{\omega}{\Lambda} \frac{2}{\ln 10} \approx 0.29\,, \tag{30}$$

where again we have assumed that $\Lambda = 3\omega$. This uncertainty estimate is required to compare theory with experiment whenever C_β is fitted to an observable.

IV. RESULTS FOR SINGLE-β DECAY

In this section we test the ET presented in Sec. III by comparing its predictions for single-β decays of odd-odd nuclei with experimental data. The ET assumes spherical symmetry for the nuclei involved in the decays, and an agreement between its predictions and experimental data complements other successful ET predictions for spectra, electromagnetic transition strengths and static moments [54, 55].

A. GT decays to excited states

We begin our calculations by studying the β decay and electron capture of spherical odd-odd parent nuclei with 1^+_{gs} ground states into different ground and excited 0^+ and 2^+ states of the even-even daughter nuclei. This will show to which extent the ET can describe processes involving individual nucleons and whether the transitions scale as expected in the ET.

For each parent nucleus, the LEC C_β can be fitted to the transition to the ground state. Then the GT decays into excited collective states are predicted by the ET according to the scaling factors in Eqs. (23) and (24):

$$\frac{|M_{\mathrm{GT}}\left(\mathrm{gs} \to 1\mathrm{ph}\right)|}{|M_{\mathrm{GT}}\left(\mathrm{gs} \to \mathrm{gs}\right)|} = \sqrt{\frac{(ft)_{\mathrm{gs-gs}}}{(ft)_{\mathrm{gs-1ph}}}} = \frac{C_{\beta 1}}{C_\beta} \approx 0.58(^{+42}_{-25})\,, \tag{31}$$

$$\frac{|M_{\mathrm{GT}}\left(\mathrm{gs} \to 2\mathrm{ph}\right)|}{|M_{\mathrm{GT}}\left(\mathrm{gs} \to \mathrm{gs}\right)|} = \sqrt{\frac{(ft)_{\mathrm{gs-gs}}}{(ft)_{\mathrm{gs-2ph}}}} = \frac{\sqrt{2} C_{\beta J_{2\mathrm{ph}} 1}}{C_\beta} \approx 0.47(^{+35}_{-20})\,. \tag{32}$$

Thus, the ET predicts equal half-lives for the decays into the even-even two-phonon states at LO. This LO result is similar to the prediction of collective models for electric quadrupole transition strengths from two-phonon states into the one-phonon state, which are predicted to be equal at low-orders. In the ET, the degeneracy is lifted at NLO. We also note that the ET naturally predicts the observed successive hindering reported in Ref. [70] of the matrix elements for GT β decays from $1^+_{\rm gs}$, $2^+_{\rm gs}$, and $3^+_{\rm gs}$ ground states of odd-odd nuclei into $0^+_{\rm gs}$, 2^+_1, and 2^+_2 states of the even-even daughter.

Figure 2 compares our ET predictions with experiment for GT β and EC decay matrix elements for a broad range of medium-mass and heavy odd-odd nuclei with mass numbers from $A = 62$ to $A = 128$. All parent nuclei have $1^+_{\rm gs}$ ground states and decay into excited 2^+_1, 0^+_2, and 2^+_2 states of the corresponding even-even nuclei. Within the ET, the 2^+_1 states are treated as one-phonon excitations of the even-even core, while the 0^+_2 and 2^+_2 states are considered to be two-phonon excitations. The ET results with uncertainties are calculated according to Eqs. (31) and (32) after adjusting the LEC C_β to the matrix element of the decay to the $0^+_{\rm gs}$ ground state of the daughter nucleus. The same figure shows that most of the experimental data, including β GT and EC decays, is consistent with the ET results. Inconsistencies are larger for the 0^+_2 and 2^+_2 two-phonon states where the ET matrix elements tend to be overestimated, especially for the β decays into 2^+_2 excited states around mass number $A \sim 110$. This is not unexpected because two-phonon states lie closer to the ET breakdown scale. In Table I, we list the values corresponding to all the theoretical and experimental matrix elements shown in Fig. 2.

B. GT decays to ground states using GT transition strengths

In Sec. IV A, we have used experimental data on single-β decays to ground states to fit the value of C_β and then predicted the matrix elements for transitions to excited states of the same nucleus. Next, we study whether it is possible to employ other data to fit the LECs and in turn predict the β-decay matrix elements to ground states.

Besides weak processes, GT strengths studied in charge-exchange reactions (via the strong interaction) are also sensitive to the GT spin-isospin operator, because the zero-degree differential cross section of the reaction is proportional to the GT strength [95]

$$S_\pm(i \to f) = |\langle f||\boldsymbol{\sigma}\tau^\pm||i\rangle|^2 \,. \qquad (33)$$

Therefore, reactions such as (p, n) or $(^3\mathrm{He}, t)$ have the same form as β^- decays, while (n, p) reactions are related to β^+-like transitions. The GT strengths and β decays of isospin-mirror nuclei have been found to be consistent in medium-mass systems [96].

In this spirit, we can use the GT transition strengths measured in $(^3\mathrm{He}, t)$ charge-exchange reactions to fit the LECs of the effective GT operator in Eq. (18). In this way, we can predict the GT matrix elements for the transition to the $0^+_{\rm gs}$ ground states of spherical even-even nuclei. Figure 3 shows that the ET results for the GT matrix elements including the theoretical uncertainty, agree very well with experiment in three of the four cases where data are available. The experimental values are calculated from the $\log(ft)$-values of the corresponding EC decays from Refs. [72, 80, 88, 93]. The remaining results in Fig. 3 show ET predictions for single-β decay of additional 1^+ states, which are, however, excited states of the odd-odd system and decay via electromagnetic transitions.

The details of the ET predictions in Fig. 3 are given in Table II, which lists the GT strengths measured in $(^3\mathrm{He}, t)$ charge-exchange reactions with initial even-even and final odd-odd nuclei for $A = 64$–130 [97–102]. For each reaction, Table II gives the experimental partial GT strength to the lowest 1^+_1 state of the odd-odd nucleus (the state expected to be well described by the ET). An exception is the case of the $^{76}\mathrm{Ge}(^3\mathrm{He}, t)^{76}\mathrm{As}$ reaction, where all the GT strength below 500 keV was taken into account (as reported in Table IV of Ref. [98]), corresponding to three close-lying 1^+ states. The resulting values for C_β fit to the partial GT strength are given in Table II including the comparison of the ET results to the experimental $\log(ft)$-values.

V. ET FOR $2\nu\beta\beta$ DECAY

In this section, we present the ET for the $2\nu\beta\beta$ decay of spherical nuclei. The decay calculations involve a sum over all 1^+ states in the intermediate odd-odd nucleus, which in general are not well described by the ET. We overcome this limitation by assuming the single-state dominance (SSD) approximation, which requires explicitly only the lowest 1^+ state. The associated uncertainty is estimated within the ET, and turns out to be comparable to the uncertainty of LO ET calculations.

A. Effective $2\nu\beta\beta$ matrix elements for decays into ground and excited states

The $2\nu\beta\beta$ decay nuclear matrix element is given in Eq. (10). Its calculation involves a sum over the contributions of all 1^+ states of the intermediate odd-odd nucleus. Since the ET is designed to reproduce only the lowest energy states of an isotope, we use the SSD approximation, which reduces the sum to the single contribution of the lowest 1^+ state. The calculation of the matrix element within the closure approximation would yield a result with a larger uncertainty estimate, as contributions from high-lying intermediate 1^+ states are not suppressed by the energy denominator. In the SSD approximation, the $2\nu\beta\beta$ decay matrix element takes the

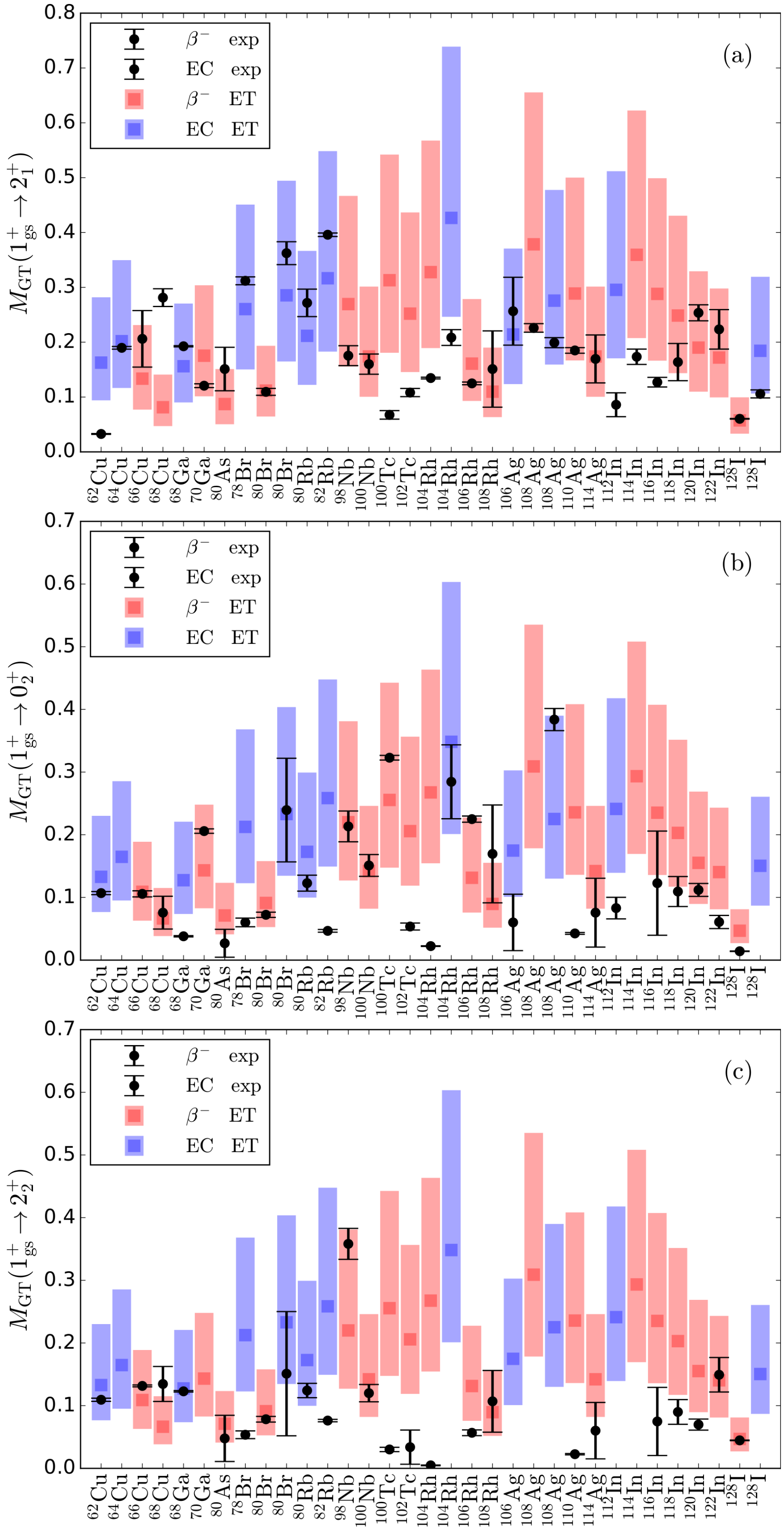

FIG. 2. Calculated ET matrix elements for GT β (red bands) and EC (blue bands) decays from parent odd-odd nuclei with 1^+_{gs} ground states into the 2^+_1 (a), 0^+_2 (b), and 2^+_2 (c) excited states of the daughter even-even nuclei, compared to experimental results (black circles) from Refs. [71–94]. For details, see Table I.

TABLE I. Experimental and calculated ET matrix elements for GT β and EC decays from parent odd-odd nuclei with $1^+_{\rm gs}$ ground states (treated as a spherical collective core coupled to a neutron and a proton) into 2^+_1 (one-phonon state), 0^+_2, and 2^+_2 (two-phonon) excited states of the daughter even-even nuclei. The LECs C_β in the effective GT operator in Eq. (18) were fitted to reproduce the log(ft) values of decays to the $0^+_{\rm gs}$ states, taking $g_A = 1.27$. The experimental values were calculated from the log(ft)-values for the transitions to the $0^+_{\rm gs}$, 2^+_1, 0^+_2, and 2^+_2 states, taken from Refs. [71–94]. The theoretical uncertainties are estimated assuming all LECs to be of natural size.

Parent → Daughter	$M_{\rm GT}\left(1^+_{\rm gs}\to 0^+_{\rm gs}\right)$		$M_{\rm GT}\left(1^+_{\rm gs}\to 2^+_1\right)$		$M_{\rm GT}\left(1^+_{\rm gs}\to 0^+_2\right)$		$M_{\rm GT}\left(1^+_{\rm gs}\to 2^+_2\right)$	
	Expt.	ET	Expt.	ET	Expt.	ET	Expt.	ET
$^{62}\text{Cu}\xrightarrow{\text{EC}}{}^{62}\text{Ni}$	0.282(1)	0.282(94)	0.033(1)	$0.163(^{+119}_{-69})$	0.107(2)	$0.133(^{+97}_{-56})$	0.109(3)	$0.133(^{+97}_{-56})$
$^{64}\text{Cu}\xrightarrow{\text{EC}}{}^{64}\text{Ni}$	0.350(2)	0.350(117)	0.190(2)	$0.202(^{+148}_{-85})$				
$^{66}\text{Cu}\xrightarrow{\beta^-}{}^{66}\text{Zn}$	0.231(14)	0.231(77)	0.206(26)	$0.134(^{+98}_{-56})$	0.106(5)	$0.109(^{+80}_{-46})$	0.132(2)	$0.109(^{+80}_{-46})$
$^{68}\text{Cu}\xrightarrow{\beta^-}{}^{68}\text{Zn}$	0.141(10)	0.141(47)	0.281(16)	$0.081(^{+60}_{-34})$	0.076(26)	$0.066(^{+49}_{-28})$	0.135(28)	$0.066(^{+49}_{-28})$
$^{68}\text{Ga}\xrightarrow{\text{EC}}{}^{68}\text{Zn}$	0.270(1)	0.270(90)	0.193(1)	$0.156(^{+114}_{-66})$	0.038(1)	$0.127(^{+93}_{-54})$	0.123(1)	$0.127(^{+93}_{-54})$
$^{70}\text{Ga}\xrightarrow{\beta^-}{}^{70}\text{Ge}$	0.304(1)	0.304(101)	0.121(3)	$0.175(^{+128}_{-74})$	0.206(4)	$0.143(^{+105}_{-61})$		$0.143(^{+105}_{-61})$
$^{80}\text{As}\xrightarrow{\beta^-}{}^{80}\text{Se}$	0.151(20)	0.151(50)	0.151(40)	$0.087(^{+64}_{-37})$	0.027(22)	$0.071(^{+52}_{-30})$	0.048(37)	$0.071(^{+52}_{-30})$
$^{78}\text{Br}\xrightarrow{\text{EC}}{}^{78}\text{Se}$	0.451(5)	0.451(150)	0.312(7)	$0.260(^{+191}_{-110})$	0.060(7)	$0.213(^{+156}_{-90})$	0.054(6)	$0.213(^{+156}_{-90})$
$^{80}\text{Br}\xrightarrow{\beta^-}{}^{80}\text{Kr}$	0.193(1)	0.193(64)	0.109(6)	$0.112(^{+82}_{-47})$	0.072(4)	$0.091(^{+67}_{-39})$	0.078(5)	$0.091(^{+67}_{-39})$
$^{80}\text{Br}\xrightarrow{\text{EC}}{}^{80}\text{Se}$	0.494(28)	0.494(165)	0.362(21)	$0.285(^{+209}_{-121})$	0.239(83)	$0.233(^{+171}_{-99})$	0.151(50)	$0.233(^{+171}_{-99})$
$^{80}\text{Rb}\xrightarrow{\text{EC}}{}^{80}\text{Kr}$	0.367(25)	0.367(122)	0.272(25)	$0.212(^{+155}_{-89})$	0.123(13)	$0.173(^{+126}_{-73})$	0.124(11)	$0.173(^{+126}_{-73})$
$^{82}\text{Rb}\xrightarrow{\text{EC}}{}^{82}\text{Kr}$	0.548(3)	0.548(183)	0.396(3)	$0.317(^{+232}_{-134})$	0.047(2)	$0.259(^{+189}_{-109})$	0.077(2)	$0.259(^{+189}_{-109})$
$^{98}\text{Nb}\xrightarrow{\beta^-}{}^{98}\text{Mo}$	0.467(32)	0.467(156)	0.175(18)	$0.269(^{+197}_{-114})$	0.213(25)	$0.220(^{+161}_{-93})$	0.358(25)	$0.220(^{+161}_{-93})$
$^{100}\text{Nb}\xrightarrow{\beta^-}{}^{100}\text{Mo}$	0.301(35)	0.301(100)	0.160(18)	$0.174(^{+127}_{-74})$	0.151(17)	$0.142(^{+104}_{-60})$	0.120(14)	$0.142(^{+104}_{-60})$
$^{100}\text{Tc}\xrightarrow{\beta^-}{}^{100}\text{Ru}$	0.542(6)	0.542(181)	0.067(8)	$0.313(^{+229}_{-132})$	0.323(4)	$0.256(^{+187}_{-108})$	0.030(2)	$0.256(^{+187}_{-108})$
$^{102}\text{Tc}\xrightarrow{\beta^-}{}^{102}\text{Ru}$	0.437(7)	0.437(146)	0.108(7)	$0.252(^{+185}_{-107})$	0.054(6)	$0.206(^{+151}_{-87})$	0.034(14)	$0.206(^{+151}_{-87})$
$^{104}\text{Rh}\xrightarrow{\beta^-}{}^{104}\text{Pd}$	0.568(7)	0.568(189)	0.135(2)	$0.328(^{+240}_{-139})$	0.022(1)	$0.268(^{+196}_{-113})$	0.005(1)	$0.268(^{+196}_{-113})$
$^{104}\text{Rh}\xrightarrow{\text{EC}}{}^{104}\text{Ru}$	0.739(1)	0.739(246)	0.208(14)	$0.427(^{+312}_{-180})$	0.285(59)	$0.348(^{+255}_{-147})$		$0.348(^{+225}_{-147})$
$^{106}\text{Rh}\xrightarrow{\beta^-}{}^{106}\text{Pd}$	0.279(2)	0.279(93)	0.125(2)	$0.161(^{+118}_{-68})$	0.225(5)	$0.131(^{+96}_{-56})$	0.057(5)	$0.131(^{+96}_{-56})$
$^{108}\text{Rh}\xrightarrow{\beta^-}{}^{108}\text{Pd}$	0.190(7)	0.190(63)	0.151(70)	$0.110(^{+80}_{-46})$	0.169(78)	$0.090(^{+66}_{-38})$	0.107(49)	$0.090(^{+66}_{-38})$
$^{106}\text{Ag}\xrightarrow{\text{EC}}{}^{106}\text{Pd}$	0.371(21)	0.371(124)	0.257(31)	$0.214(^{+157}_{-90})$	0.060(22)	$0.175(^{+128}_{-74})$		$0.175(^{+128}_{-74})$
$^{108}\text{Ag}\xrightarrow{\beta^-}{}^{108}\text{Cd}$	0.656(7)	0.656(219)	0.226(8)	$0.378(^{+277}_{-160})$				
$^{108}\text{Ag}\xrightarrow{\text{EC}}{}^{108}\text{Pd}$	0.478(16)	0.478(159)	0.199(9)	$0.276(^{+202}_{-117})$	0.384(18)	$0.225(^{+165}_{-95})$		$0.225(^{+165}_{-95})$
$^{110}\text{Ag}\xrightarrow{\beta^-}{}^{110}\text{Cd}$	0.500(2)	0.500(167)	0.186(5)	$0.289(^{+211}_{-122})$	0.043(1)	$0.236(^{+173}_{-100})$	0.023(1)	$0.236(^{+173}_{-100})$
$^{114}\text{Ag}\xrightarrow{\beta^-}{}^{114}\text{Cd}$	0.301(18)	0.301(100)	0.169(22)	$0.174(^{+127}_{-74})$	0.076(27)	$0.142(^{+104}_{-60})$	0.060(22)	$0.142(^{+104}_{-60})$
$^{112}\text{In}\xrightarrow{\text{EC}}{}^{112}\text{Cd}$	0.512(35)	0.512(171)	0.086(22)	$0.295(^{+216}_{-125})$	0.083(17)	$0.241(^{+177}_{-102})$		$0.241(^{+177}_{-102})$
$^{114}\text{In}\xrightarrow{\beta^-}{}^{114}\text{Sn}$	0.622(1)	0.622(207)	0.173(14)	$0.359(^{+263}_{-152})$				
$^{116}\text{In}\xrightarrow{\beta^-}{}^{116}\text{Sn}$	0.499(3)	0.499(166)	0.127(9)	$0.288(^{+211}_{-122})$	0.123(42)	$0.235(^{+172}_{-99})$	0.075(27)	$0.235(^{+172}_{-99})$
$^{118}\text{In}\xrightarrow{\beta^-}{}^{118}\text{Sn}$	0.431(15)	0.431(144)	0.164(34)	$0.249(^{+182}_{-105})$	0.109(24)	$0.203(^{+149}_{-86})$	0.090(20)	$0.203(^{+149}_{-86})$
$^{120}\text{In}\xrightarrow{\beta^-}{}^{120}\text{Sn}$	0.329(8)	0.329(110)	0.254(15)	$0.190(^{+139}_{-80})$	0.112(10)	$0.155(^{+114}_{-66})$	0.070(9)	$0.155(^{+114}_{-66})$
$^{122}\text{In}\xrightarrow{\beta^-}{}^{122}\text{Sn}$	0.298(34)	0.298(99)	0.223(36)	$0.172(^{+126}_{-73})$	0.061(11)	$0.140(^{+103}_{-59})$	0.149(28)	$0.140(^{+103}_{-59})$
$^{128}\text{I}\xrightarrow{\beta^-}{}^{128}\text{Xe}$	0.099(1)	0.099(33)	0.060(1)	$0.057(^{+42}_{-24})$	0.014(1)	$0.047(^{+34}_{-20})$	0.045(1)	$0.047(^{+34}_{-20})$
$^{128}\text{I}\xrightarrow{\text{EC}}{}^{128}\text{Te}$	0.319(18)	0.319(106)	0.106(7)	$0.184(^{+135}_{-78})$				

TABLE II. Selected (^{3}He, t) charge-exchange reactions (first column), experimental partial GT strengths (second column) from Refs. [97–102], and C_β values fitted to them (third column). The fourth and fifth columns compare the experimental and ET results for the log(ft) values of the corresponding EC decays, where the experimental values are taken from Refs. [72, 80, 88, 93].

Reaction	$S(0^+_{\rm gs}\to 1^+_1)$	C_β	log(ft)	
			Expt.	ET
^{64}Ni(^{3}He, t)^{64}Cu	0.123	0.202	4.97	4.97(29)
^{76}Ge(^{3}He, t)^{76}As[a]	0.210	0.265		4.74(29)
^{82}Se(^{3}He, t)^{82}Br	0.338	0.336		4.53(29)
^{100}Mo(^{3}He, t)^{100}Tc	0.348	0.341	4.40	4.51(29)
^{116}Cd(^{3}He, t)^{116}In	0.032	0.103	4.47	5.55(29)
^{128}Te(^{3}He, t)^{128}I	0.079	0.162	5.05	5.16(29)
^{130}Te(^{3}He, t)^{130}I	0.072	0.155		5.20(29)

[a] Comprises the sum of GT strength below 500 keV, see text.

form

$$M^{2\nu\beta\beta}_{\rm GT}(0^+_{\rm gs}\to f)\approx\frac{M_{\rm GT}(1^+_1\to f)M_{\rm GT}(0^+_{\rm gs}\to 1^+_1)}{\sqrt{s}(D_{1f}/m_e)^s}$$
$$=\frac{3\kappa}{\sqrt{s}g_A^2}\left(\frac{m_e}{D_{1f}}\right)^s\sqrt{\frac{1}{(ft)_{1^+_1 f}(ft)_{1^+_1 0^+_{\rm gs}}}}\,, \tag{34}$$

where $s\equiv 1+2\delta_{2J_f}$, and we have written the latter in terms of the matrix elements (or ft values) of single-β decays or charge-exchange reactions, calculated in Sec. IV.

First, we focus on transitions to the ground state of the final nucleus. We can estimate the uncertainty associated

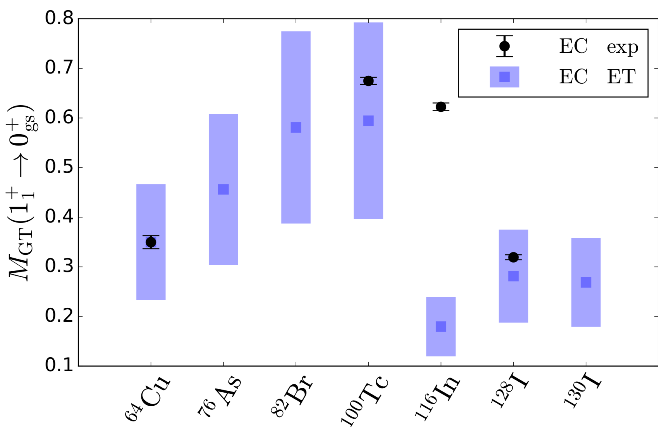

FIG. 3. Calculated GT matrix elements for the transition from the 1^+_1 states of odd-odd nuclei to the $0^+_{\rm gs}$ ground states of even-even nuclei, using as ET input the GT transition strengths measured in (^{3}He, t) charge-exchange reactions (blue bands), see also Table II. The ET results are compared to experiment calculated from the log(ft)-values of the corresponding EC decays (black circles) from Refs. [72, 80, 88, 93].

with the SSD approximation within the ET, as low-lying 1^+ states of the odd-odd system are decribed as multiphonon excitations of the lowest 1^+ state at LO. Thus, their energies and GT matrix elements are expected to be

$$E(1^+_{n+1})\sim E(1^+_1)+n\omega\,, \tag{35}$$

$$M_{\rm GT}\left(0^+_{\rm gs}\to 1^+_{n+1}\right)\sim\left(\frac{\omega}{\Lambda}\right)^{n/2}M_{\rm GT}\left(0^+_{\rm gs}\to 1^+_1\right)\,, \tag{36}$$

according to the power counting introduced in Eq. (22). Under these assumptions, the uncertainty in the $2\nu\beta\beta$ decay matrix element for the transition to the $0^+_{\rm gs}$ state due to the SSD approximation scales as

$$\Delta M^{2\nu\beta\beta}_{\rm GT}(0^+_{\rm gs}\to 0^+_{\rm gs})$$
$$\sim\sum_{n=1}\left(\frac{\omega}{\Lambda}\right)^n\frac{M_{\rm GT}(1^+_1\to 0^+_{\rm gs})M_{\rm GT}(0^+_{\rm gs}\to 1^+_1)}{(D_{10^+_{\rm gs}}+n\omega)/m_e} \tag{37}$$
$$=\frac{D_{10^+_{\rm gs}}}{\Lambda}\Phi\left(\frac{\omega}{\Lambda},1,\frac{D_{10^+_{\rm gs}}+\omega}{\omega}\right)M^{2\nu}_{\rm GT}(0^+_{\rm gs}\to 0^+_{\rm gs})\,,$$

where

$$\Phi(z,s,a)\equiv\sum_{n=0}^{\infty}\frac{z^n}{(a+n)^s}\,, \tag{38}$$

is the Lerch transcendent. The relative uncertainty δ is

$$\delta(\text{gs}\to\text{gs})=\frac{D_{10^+_{\rm gs}}}{\Lambda}\Phi\left(\frac{\omega}{\Lambda},1,\frac{D_{10^+_{\rm gs}}+\omega}{\omega}\right)\,. \tag{39}$$

Whether this systematic error due to the SSD approximation is smaller or larger than the uncertainty associated with the order at which the matrix elements are calculated depends on the energy scales ω, Λ and $D_{10^+_{\rm gs}}$.

Similarly to single-β decays, we can also calculate the matrix elements for $2\nu\beta\beta$ decays into 0^+_2 excited states within the ET. Figure 4 shows a diagram with the relevant energy scales of the nuclei involved. In this case, the SSD approximation is not expected to work so well, because the contributions from the second and third 1^+ states ($n=2,3$) in

$$M^{2\nu\beta\beta}_{\rm GT}(0^+_{\rm gs}\to 0^+_2)=\sum_{n=1}\frac{M_{\rm GT}(1^+_n\to 0^+_2)M_{\rm GT}(0^+_{\rm gs}\to 1^+_n)}{D_{n0^+_2}/m_e}\,, \tag{40}$$

contain the same number of d operators as the first term. Thus, based on the power counting in Eq. (22), the first three terms are expected to scale similarly. Nevertheless, if only the first term in Eq. (40) is considered, the $2\nu\beta\beta$ decay matrix element takes the approximate form

$$M^{2\nu\beta\beta}_{\rm GT}(0^+_{\rm gs}\to 0^+_2)\approx\frac{M_{\rm GT}(1^+_{\rm gs}\to 0^+_2)M_{\rm GT}(0^+_{\rm gs}\to 1^+_1)}{D_{10^+_2}/m_e}$$
$$\approx\frac{D_{10^+_{\rm gs}}}{D_{10^+_2}}\frac{M_{\rm GT}(1^+_1\to 0^+_2)}{M_{\rm GT}(1^+_1\to 0^+_{\rm gs})}M^{2\nu}_{\rm GT}(0^+_{\rm gs}\to 0^+_{\rm gs})\,, \tag{41}$$

with a relative uncertainty

$$\delta(\mathrm{gs}\to 0_2^+) = \frac{D_{10_2^+}}{D_{20_2^+}}+\frac{D_{10_2^+}}{D_{30_2^+}}+\frac{D_{10_2^+}}{\Lambda}\Phi\left(\frac{\omega}{\Lambda},1,\frac{D_{30_2^+}+\omega}{\omega}\right). \tag{42}$$

We can reduce this relative uncertainty assuming that the contributions due to the first three terms are in phase. This yields the following matrix element

$$M_{\mathrm{GT}}^{2\nu\beta\beta}(0_{\mathrm{gs}}^+\to 0_2^+)\approx\left(1+\frac{D_{10_2^+}}{D_{20_2^+}}+\frac{D_{10_2^+}}{D_{30_2^+}}\right)\times\frac{D_{10_{\mathrm{gs}}^+}}{D_{10_2^+}}\frac{M_{\mathrm{GT}}(1_1^+\to 0_2^+)}{M_{\mathrm{GT}}(1_1^+\to 0_{\mathrm{gs}}^+)}M_{\mathrm{GT}}^{2\nu\beta\beta}(0_{\mathrm{gs}}^+\to 0_{\mathrm{gs}}^+)\,, \tag{43}$$

and the reduced relative uncertainty

$$\delta(\mathrm{gs}\to 0_2^+) =\frac{\omega}{\Lambda}\left(\frac{D_{10_2^+}}{D_{20_2^+}}+\frac{D_{10_2^+}}{D_{30_2^+}}\right)+\frac{D_{10_2^+}}{\Lambda}\Phi\left(\frac{\omega}{\Lambda},1,\frac{D_{30_2^+}+\omega}{\omega}\right). \tag{44}$$

In Sec. V B, we compare to experimental results the $2\nu\beta\beta$ matrix element of ^{100}Mo decaying into the 0_2^+ state of ^{100}Ru using Eqs. (41) and (43), with the uncertainties given by Eqs. (42) and (44).

The ET can also predict $2\nu\beta\beta$ decays matrix elements to excited 2_1^+ states of the daughter nucleus. Here, because energy denominators appear to the third power, we only consider the contribution due to the first intermediate 1^+ state. Then, matrix elements for decays into 2_1^+ states take the approximate form

$$M_{\mathrm{GT}}^{2\nu\beta\beta}(0_{\mathrm{gs}}^+\to 2_1^+)\approx\sqrt{\frac{1}{3}\frac{m_e^2 D_{10_{\mathrm{gs}}^+}}{D_{12_1^+}^3}}\frac{M_{\mathrm{GT}}(1_1^+\to 2_1^+)}{M_{\mathrm{GT}}(1_1^+\to 0_{\mathrm{gs}}^+)}M_{\mathrm{GT}}^{2\nu\beta\beta}(0_{\mathrm{gs}}^+\to 0_{\mathrm{gs}}^+), \tag{45}$$

with an associated relative uncertainty given by

$$\delta(\mathrm{gs}\to 2_1^+) =\frac{D_{12_1^+}^3}{\omega^3}\Phi\left(\frac{\omega}{\Lambda},3,\frac{D_{12_1^+}+\omega}{\omega}\right). \tag{46}$$

This uncertainty varies from nucleus to nucleus, depending on the energy scales ω and $D_{12_1^+}$.

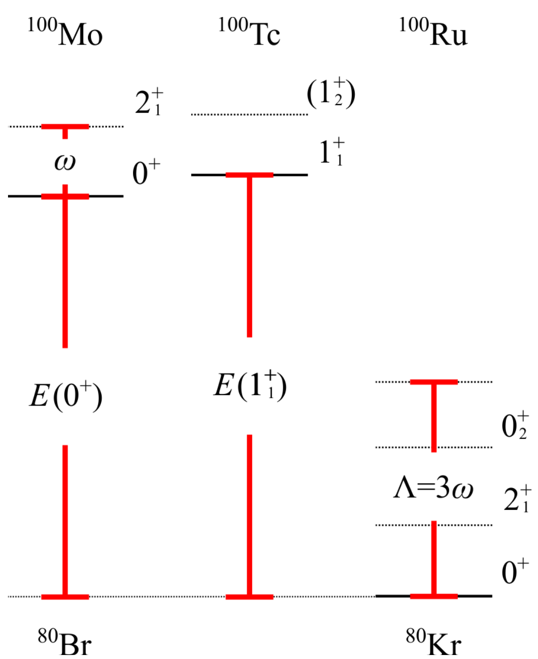

FIG. 4. Energy scales relevant to the $2\nu\beta\beta$ decay matrix element from the 0_{gs}^+ ground state of the parent nucleus ^{100}Mo via the 1^+ intermediate states in ^{100}Tc to the 0_{gs}^+ ground state and 0_2^+ excited state of the daughter nucleus ^{100}Ru.

B. Results for $2\nu\beta\beta$ decay

As an example, let us first focus on the ^{100}Mo $2\nu\beta\beta$ decay. The relevant energy scales are shown in Fig. 4. Setting the energy scale ω equal to the average of the excitation energies of the 2_1^+ states in the even-even nuclei and the breakdown scale to $\Lambda = 3\omega$, Eqs. (34) and (39) yield for the decay to the ^{100}Ru ground state

$$M_{\mathrm{GT}}^{2\nu\beta\beta}(0_{\mathrm{gs}}^+\to 0_{\mathrm{gs}}^+)\approx 0.111(38)\,, \tag{47}$$

where we have fitted the LECs of the ET to the experimental single-β and EC decays and the uncertainty given is thus dominated by the SSD approximation from Eq. (39). We note that the uncertainty due to the SSD approximation (35% in this case) is of the same order as the uncertainty associated with the effective nuclear states and GT operator used to calculate the single-β decay matrix elements at LO. Therefore, the SSD approximation is appropriate to obtain $2\nu\beta\beta$ decay matrix elements at LO.

Figure 5 shows the ET results for the $2\nu\beta\beta$ and 2νECEC decays of several nuclei with mass number from $A = 64$ to $A = 130$. The LECs of the ET are again fitted to experimental single-β and/or EC decays, or to GT strengths if the former are not available. The results, as well as the GT matrix elements used for both single-β decay branches, are also given in Table III. In some cases, for which there is no experimental data on single-β decay, EC decay or GT strengths, the GT matrix elements were assumed to be similar for both β decay branches, as indicated in Table III. The similarity of the two matrix elements is a prediction of the ET. The top panel in Fig. 5 shows that the theoretical results with uncertainties for decays to the ground state of the daughter nucleus agree remarkably well with experimental data when available. We provide additional ET predictions for the kinematically less favored $2\nu\beta\beta$ decays and 2νECEC transitions. While the $2\nu\beta\beta$ decays from ^{48}Ca, ^{96}Zr, ^{136}Xe, and ^{150}Nd

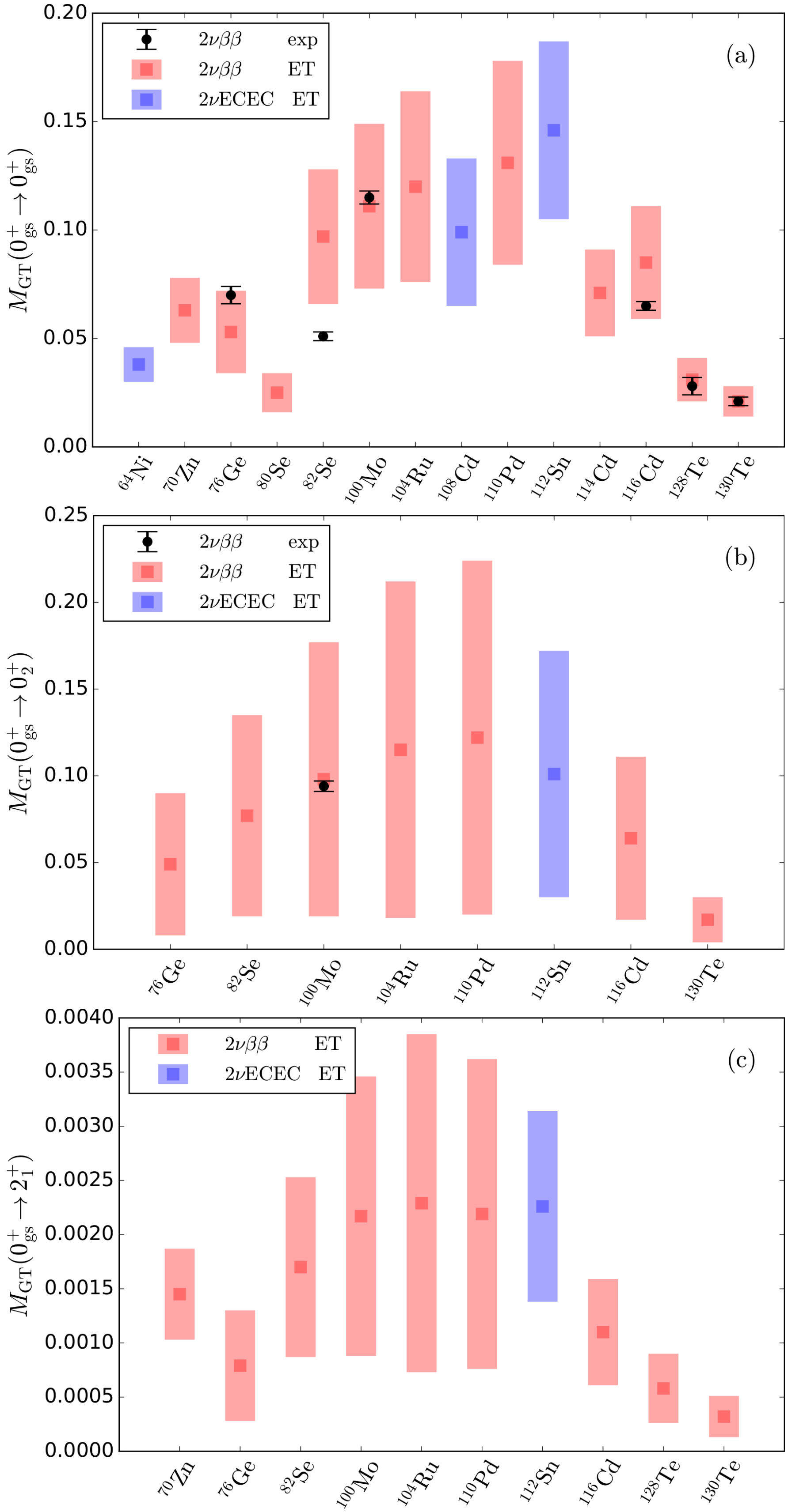

FIG. 5. Calculated ET matrix elements for $2\nu\beta\beta$ (red bands) and 2νECEC (blue bands) decays to low-lying collective ground (a) and excited 0^+_2 (b) and 2^+_1 (c) states of the daughter nuclei, in comparison with experiment (black bars). The LECs of the ET are fitted to single-β and/or EC decays (or to GT strengths if the former are not available) The experimental matrix elements are taken from Ref. [26].

TABLE III. $2\nu\beta\beta$ and 2νECEC matrix elements for the decays to low-lying collective states of the daughter nuclei. The values for the LEC ω are listed in the second column. The LECs of the effective GT operator are fitted to reproduce the matrix elements for single-β and/or EC decays, or GT strengths from charge-exchange reactions if the former are not available (third and fourth columns). Calculated decays into ground states (sixth column) assume the SSD approximation, while decays to 0_2^+ (eighth column) and 2_1^+ (nineth column) excited states are calculated according to Eqs. (43) and (44) and Eqs. (45) and (46), respectively. Experimental data for decays to ground (fifth column) and excited (seventh column) 0^+ states are taken from Ref. [26].

Decay	ω[keV]	$M_{\rm GT}$		$M_{\rm GT}^{2\nu\beta\beta/{\rm ECEC}}(0^+_{\rm gs}\to 0^+_{\rm gs})$		$M_{\rm GT}^{2\nu\beta\beta/{\rm ECEC}}(0^+_{\rm gs}\to 0^+_2)$		$M_{\rm GT}^{2\nu\beta\beta/{\rm ECEC}}(0^+_{\rm gs}\to 2^+_1)$
		$(0^+_{\rm gs}\to 1^+_1)$	$(1^+_1\to 0^+_{\rm gs})$	Expt.	ET	Expt.	ET	ET
$^{64}{\rm Zn}\xrightarrow{\rm ECEC}{}^{64}{\rm Ni}$	1168.7	0.239	0.350		0.038(8)			
$^{70}{\rm Zn}\xrightarrow{\beta^-\beta^-}{}^{70}{\rm Ge}$	962.2	0.467	0.304		0.063(15)			0.00145(42)
$^{76}{\rm Ge}\xrightarrow{\beta^-\beta^-}{}^{76}{\rm Se}$	561.0	0.456[a]	0.456[b]	0.070(4)	0.053(19)		0.049(41)	0.00079(51)
$^{80}{\rm Se}\xrightarrow{\beta^-\beta^-}{}^{80}{\rm Kr}$	641.4	0.494	0.193		0.025(9)			
$^{82}{\rm Se}\xrightarrow{\beta^-\beta^-}{}^{82}{\rm Kr}$	715.6	0.581[a]	0.548[c]	0.051(2)	0.097(31)		0.077(58)	0.00170(83)
$^{100}{\rm Mo}\xrightarrow{\beta^-\beta^-}{}^{100}{\rm Ru}$	537.5	0.675	0.542	0.115(3)	0.111(38)	0.094(3)	0.098(79)	0.00217(129)
$^{104}{\rm Ru}\xrightarrow{\beta^-\beta^-}{}^{104}{\rm Pd}$	456.9	0.740	0.568		0.120(44)		0.115(97)	0.00229(156)
$^{106}{\rm Cd}\xrightarrow{\rm ECEC}{}^{106}{\rm Pd}$	572.2	$<$0.953	0.371		$<$0.114(38)		$<$0.097(76)	$<$0.00243(133)
$^{108}{\rm Cd}\xrightarrow{\rm ECEC}{}^{108}{\rm Pd}$	533.4	0.655	0.478		0.099(34)			
$^{110}{\rm Pd}\xrightarrow{\beta^-\beta^-}{}^{110}{\rm Cd}$	515.8	0.964	0.500		0.131(47)		0.122(102)	0.00219(143)
$^{112}{\rm Sn}\xrightarrow{\rm ECEC}{}^{112}{\rm Cd}$	937.1	0.910	0.512		0.146(41)		0.101(71)	0.00226(88)
$^{114}{\rm Cd}\xrightarrow{\beta^-\beta^-}{}^{114}{\rm Sn}$	929.2	0.384	0.622		0.071(20)			
$^{116}{\rm Cd}\xrightarrow{\beta^-\beta^-}{}^{116}{\rm Sn}$	903.5	0.622	0.499	0.065(2)	0.085(26)		0.064(47)	0.00110(49)
$^{128}{\rm Te}\xrightarrow{\beta^-\beta^-}{}^{128}{\rm Xe}$	593.0	0.319	0.319[d]	0.028(4)	0.031(10)			0.00058(32)
$^{130}{\rm Te}\xrightarrow{\beta^-\beta^-}{}^{130}{\rm Xe}$	687.8	0.269[a]	0.269[e]	0.021(2)	0.021(7)		0.017(13)	0.00036(19)

[a] Calculated with LECs fitted to charge-exchange reactions.
[b] Assumed similar to the $^{76}{\rm Ge}\to{}^{76}{\rm As}$ matrix element.
[c] Assumed similar to the $^{82}{\rm Rb}\to{}^{82}{\rm Kr}$ matrix element.
[d] Assumed similar to the $^{128}{\rm I}\to{}^{128}{\rm Te}$ matrix element.
[e] Assumed similar to the $^{130}{\rm I}\to{}^{130}{\rm Te}$ matrix element.

have been measured, they are not included in our comparison because their low-energy properties, or those of the corresponding daughter nuclei, do not resemble those expected for collective spherical systems.

The middle panel of Fig. 5 shows predicted ET matrix elements for $2\nu\beta\beta$ decays into energetically allowed 0_2^+ states. The matrix elements, calculated with Eq. (43), are listed in Table III. The ET uncertainties are larger than those for decays to the ground state because of the larger impact of high-energy 1^+ states. Nonetheless, the predicted matrix elements for transitions to excited 0_2^+ and the ground state are similar.

It is especially interesting to compare to the measured ^{100}Mo decay into the 0_2^+ state of ^{100}Ru. In this case the SSD approximation given by Eqs. (41) and (42) yields

$$M_{\rm GT}^{2\nu\beta\beta}(0_{\rm gs}^+ \to 0_2^+) \approx 0.040(71)\,, \tag{48}$$

which clearly shows (the relative error reaches 180%) that the contributions from the second and third 1^+ states in the sum in Eq. (40) cannot be neglected. When we take these two additional terms into account and assume that the first three contributions add up with the same phase, the $2\nu\beta\beta$ matrix element given by Eqs. (43) and (44) becomes

$$M_{\rm GT}^{2\nu\beta\beta}(0_{\rm gs}^+ \to 0_2^+) \approx 0.098(79)\,, \tag{49}$$

with a smaller but still significant relative uncertainty of 80%. We note that the two ET results are consistent with the experimental value $M_{\rm GT}^{2\nu\beta\beta}(0_{\rm gs}^+ \to 0_2^+) = 0.094(3)$. The agreement with the result yielded by Eq. (43) suggests that for this transition the contributions from the first three 1^+ states in Eq. (40) likely add up in phase.

The bottom panel of Fig. 5 shows the ET predictions for matrix elements of decays into excited 2_1^+ states, calculated using Eqs. (45) and (46). The values with corresponding uncertainties are listed in Table III. The higher power of the energy denominator compared to decays to 0^+ states suppresses the matrix elements into 2_1^+ states. Not a single transition of this type has been detected experimentally. On the other hand, the expected dominance of the transition through the lowest 1^+ state in the intermediate nucleus reduces the ET uncertainties with respect to transitions to excited 0_2^+ states.

The LO $2\nu\beta\beta$ and 2νECEC results can be systematically improved, and the uncertainties reduced, at higher orders in the ET. The cost is to introduce additional LECs that need to be fitted to data on the energy spectra, β^- and EC decays of the intermediate odd-odd nuclei.

VI. SUMMARY AND OUTLOOK

We have studied β and EC decays within an ET that treats nuclei as a spherical even-even core that can be coupled to one additional neutron and/or proton. By fitting the LEC of the effective GT operator to the decay to the ground state of the daughter nucleus, the matrix elements corresponding to the decays to collective excited states of the same nucleus are predicted by the ET. We have also used experimental data on charge-exchange reactions to fit the LECs and predict the decay into the daughter ground state. One of the advantages of the ET is that it provides a power counting that allow us to estimate the theoretical uncertainty of the calculations. When this uncertainty is included, we find good agreement between the ET predictions and experiment. The consistency covers more than 20 spherical medium-mass and heavy nuclei. Our results thus suggest that transitions due to the weak interactions can be well described by the ET at LO.

In addition, we have used data on single-β and/or EC decays, or GT strengths from charge-exchange reactions, to calculate matrix elements for $2\nu\beta\beta$ and 2νECEC decays. We generally assume the SSD approximation, which is consistent with obtaining results with the ET at LO. Without modifying the LECs of the first-order processes, the ET gives $2\nu\beta\beta$ decay matrix elements consistent with experiment. In one case the agreement extends to the $2\nu\beta\beta$ decay into an excited 0_2^+ state. Furthermore, we have predicted several $2\nu\beta\beta$ and 2νECEC matrix elements into ground and excited 0_2^+ and 2_1^+ states. Based on the power counting of the ET, the LO matrix elements to ground and excited states are predicted consistently. The validity of the ET will be challenged when future experiments measure these transitions.

Future work includes a more precise ET calculation. This will require us to include higher-order corrections to the Hamiltonian for the odd-odd nuclei, which will in turn correct our LO approximation for the low-lying odd-odd states, as well as higher-order corrections to the effective GT operator. Based on the power counting, we expect these two kinds of corrections to contribute a factor of $\omega/\Lambda \sim 30\%$ to the reduced GT matrix elements for $2\nu\beta\beta$ decays. Work in these directions is in progress.

In addition, it will be important to perform LO calculations within ETs for axial [49–52] and triaxial [103] nuclei. This will provide access to nuclei whose ground states deviate from sphericity, and is thus also expected to improve the calculations for some nuclei in this work, whose ground states possess some deformation.

An extension of the ET presented here is also a promising framework to estimate the matrix elements of $0\nu\beta\beta$ decays with theoretical uncertainties. For this purpose, the effective $0\nu\beta\beta$ decay operator needs to be written in terms of the DOF of the ET, and the corresponding LECs would have to be fixed. Since there is no experimental data on $0\nu\beta\beta$ decay yet, the fitting of the LECs can be validated against other experimental data strongly correlated to $0\nu\beta\beta$ decay. Alternatively, the ET LECs can be fitted to existing nuclear structure calculations, which is similar to the strategy followed by interacting boson model calculations (see, e.g., Ref. [104]). Both strategies will provide constraints and predictions for the $0\nu\beta\beta$ matrix elements with ET uncertainties.

ACKNOWLEDGMENTS

We thank T. Papenbrock for very useful comments on the manuscript. This work was supported in part by the Deutsche Forschungsgesellschaft under Grant SFB 1245, MEXT, as Priority Issue on Post-K Computer (Elucidation of the Fundamental Laws and Evolution of the Universe), and JICFuS.

---

[1] N. Severijns and O. Naviliat-Cuncic, "Symmetry tests in nuclear beta decay," Annu. Rev. Nucl. Part. Sci. **61**, 23 (2011).

[2] L. Baudis, "Direct dark matter detection: the next decade," Phys. Dark Univ. **1**, 94 (2012), 1211.7222.

[3] J. Engel, M. J. Ramsey-Musolf, and U. van Kolck, "Electric dipole moments of nucleons, nuclei, and atoms: The standard model and beyond," Prog. Part. Nucl. Phys. **71**, 21 (2013).

[4] K. Langanke and G. Martínez-Pinedo, "Nuclear weak interaction processes in stars," Rev. Mod. Phys. **75**, 819 (2003).

[5] M. Arnould, S. Goriely, and K. Takahashi, "The r-process of stellar nucleosynthesis: Astrophysics and nuclear physics achievements and mysteries," Phys. Rept. **450**, 97 (2007).

[6] A. Arcones and F. K. Thielemann, "Neutrino-driven wind simulations and nucleosynthesis of heavy elements," J. Phys. G **40**, 013201 (2013).

[7] D. Gazit, S. Quaglioni, and P. Navrátil, "Three-nucleon low-energy constants from the consistency of interactions and currents in chiral effective field theory," Phys. Rev. Lett. **103**, 102502 (2009).

[8] A. Baroni, L. Girlanda, A. Kievsky, L. E. Marcucci, R. Schiavilla, and M. Viviani, "Tritium β decay in chiral effective field theory," Phys. Rev. C **94**, 024003 (2016).

[9] P. Klos, A. Carbone, K. Hebeler, J. Menéndez, and A. Schwenk, "Uncertainties in constraining low-energy constants from ^{3}H β decay," Eur. Phys. J. A **53**, 168 (2017).

[10] P. Maris, J. P. Vary, P. Navrátil, W. E. Ormand, H. Nam, and D. J. Dean, "Origin of the anomalous long lifetime of ^{14}C," Phys. Rev. Lett. **106**, 202502 (2011).

[11] A. Ekström, G. R. Jansen, K. A. Wendt, G. Hagen, T. Papenbrock, S. Bacca, B. Carlsson, and D. Gazit, "Effects of three-nucleon forces and two-body currents on Gamow-Teller strengths," Phys. Rev. Lett. **113**, 262504 (2014).

[12] T. Nikšić, T. Marketin, D. Vretenar, N. Paar, and P. Ring, "β-decay rates of r-process nuclei in the relativistic quasiparticle random phase approximation," Phys. Rev. C **71**, 014308 (2005).

[13] T. Marketin, D. Vretenar, and P. Ring, "Calculation of β-decay rates in a relativistic model with momentum-dependent self-energies," Phys. Rev. C **75**, 024304 (2007).

[14] Z. M. Niu, Y. F. Niu, H. Z. Liang, W. H. Long, T. Nikšić, D. Vretenar, and J. Meng, "β-decay half-lives of neutron-rich nuclei and matter flow in the r-process," Phys. Lett. B **723**, 172 (2013).

[15] Z. M. Niu, Y. F. Niu, Q. Liu, H. Z. Liang, and J. Y. Guo, "Nuclear β^{+}/EC decays in covariant density functional theory and the impact of isoscalar proton-neutron pairing," Phys. Rev. C **87**, 051303 (2013).

[16] D.-L. Fang, B. A. Brown, and T. Suzuki, "Investigating β-decay properties of spherical nuclei along the possible r-process path," Phys. Rev. C **88**, 034304 (2013).

[17] M. T. Mustonen, T. Shafer, Z. Zenginerler, and J. Engel, "Finite-amplitude method for charge-changing transitions in axially-deformed nuclei," Phys. Rev. C **90**, 024308 (2014).

[18] T. Shafer, J. Engel, C. Fröhlich, G. C. McLaughlin, M. Mumpower, and R. Surman, "β decay of deformed r-process nuclei near A=80 and A=160, including odd-A and odd-odd nuclei, with the Skyrme finite-amplitude method," Phys. Rev. C **94**, 055802 (2016).

[19] P. Möller, B. Pfeiffer, and K.-L. Kratz, "New calculations of gross β-decay properties for astrophysical applications: Speeding up the classical r-process," Phys. Rev. C **67**, 055802 (2003).

[20] E. Caurier, G. Martínez-Pinedo, F. Nowacki, A. Poves, and A. P. Zuker, "The shell model as unified view of nuclear structure," Rev. Mod. Phys. **77**, 427 (2005).

[21] T. Suzuki, T. Yoshida, T. Kajino, and T. Otsuka, "β decays of isotones with neutron magic number of $N=126$ and r-process nucleosynthesis," Phys. Rev. C **85**, 015802 (2012).

[22] Q. Zhi, E. Caurier, J. J. Cuenca-García, K. Langanke, G. Martínez-Pinedo, and K. Sieja, "Shell-model half-lives including first-forbidden contributions for r-process waiting-point nuclei," Phys. Rev. C **87**, 025803 (2013).

[23] V. Kumar, P. C. Srivastava, and H. Li, "Nuclear β^{-}-decay half-lives for fp and fpg shell nuclei," J. Phys. G **43**, 105104 (2016).

[24] B. A. Brown and B. H. Wildenthal, "Status of the nuclear shell model," Annu. Rev. Nucl. Part. Sci. **38**, 29 (1988).

[25] G. Martínez-Pinedo, A. Poves, E. Caurier, and A. P. Zuker, "Effective g_A in the pf shell," Phys. Rev. C **53**, R2602 (1996).

[26] A. S. Barabash, "Average and recommended half-life values for two-neutrino double beta decay," Nucl. Phys. A **935**, 52 (2015).

[27] M. Agostini *et al.* (GERDA Collaboration), "Background-free search for neutrinoless double-β decay of ^{76}Ge with GERDA," Nature **544**, 47 (2017).

[28] A. Gando *et al.* (KamLAND-Zen Collaboration), "Search for Majorana neutrinos near the inverted mass hierarchy region with KamLAND-Zen," Phys. Rev. Lett. **117**, 082503 (2016).

[29] K. Alfonso *et al.* (CUORE Collaboration), "Search for neutrinoless double-beta decay of ^{130}Te with CUORE-0," Phys. Rev. Lett. **115**, 102502 (2015).

[30] J. B. Albert *et al.* (EXO-200 Collaboration), "Search for Majorana neutrinos with the first two years of EXO-200 data," Nature **510**, 229 (2014).

[31] E. Caurier, F. Nowacki, and A. Poves, "Shell model description of the $\beta\beta$ decay of ^{136}Xe," Phys. Lett. B **711**, 62 (2012).

[32] J. D. Vergados, H. Ejiri, and F. Šimkovic, "Theory of neutrinoless double-beta decay," Rept. Prog. Phys. **75**, 106301 (2012).

[33] J. Suhonen and O. Civitarese, "Double-beta-decay nuclear matrix elements in the QRPA framework," J. Phys. G **39**, 085105 (2012).

[34] J. Engel and J. Menéndez, "Status and future of nuclear matrix elements for neutrinoless double-beta decay: A review," Rept. Prog. Phys. **80**, 046301 (2017).

[35] J. Dobaczewski, W. Nazarewicz, and P.-G. Reinhard, "Error estimates of theoretical models: A guide," J. Phys. G **41**, 074001 (2014).

[36] R. J. Furnstahl, D. R. Phillips, and S. Wesolowski, "A recipe for EFT uncertainty quantification in nuclear physics," J. Phys. G **42**, 034028 (2015).

[37] R. J. Furnstahl, N. Klco, D. R. Phillips, and S. Wesolowski, "Quantifying truncation errors in effective field theory," Phys. Rev. C **92**, 024005 (2015).

[38] S. Wesolowski, N. Klco, R. J. Furnstahl, D. R. Phillips, and A. Thapaliya, "Bayesian parameter estimation for effective field theories," J. Phys. G **43**, 074001 (2016).

[39] U. van Kolck, "Effective field theory of nuclear forces," Prog. Part. Nucl. Phys. **43**, 337 (1999).

[40] P. F. Bedaque and U. van Kolck, "Effective field theory for few-nucleon systems," Annu. Rev. Nucl. Part. Sci. **52**, 339 (2002).

[41] E. Epelbaum, H.-W. Hammer, and U.-G. Meißner, "Modern theory of nuclear forces," Rev. Mod. Phys. **81**, 1773 (2009).

[42] R. Machleidt and D. R. Entem, "Chiral effective field theory and nuclear forces," Phys. Rept. **503**, 1 (2011).

[43] H.-W. Hammer, A. Nogga, and A. Schwenk, "Three-body forces: From cold atoms to nuclei," Rev. Mod. Phys. **85**, 197 (2013).

[44] B. R. Barrett, P. Navrátil, and J. P. Vary, "*Ab initio* no core shell model," Prog. Part. Nucl. Phys. **69**, 131 (2013).

[45] G. Hagen, T. Papenbrock, M. Hjorth-Jensen, and D. J. Dean, "Coupled-cluster computations of atomic nuclei," Rept. Prog. Phys. **77**, 096302 (2014).

[46] K. Hebeler, J. D. Holt, J. Menéndez, and A. Schwenk, "Nuclear forces and their impact on neutron-rich nuclei and neutron-rich matter," Annu. Rev. Nucl. Part. Sci. **65**, 457 (2015).

[47] P. Navrátil, S. Quaglioni, G. Hupin, C. Romero-Redondo, and A. Calci, "Unified *ab initio* approaches to nuclear structure and reactions," Phys. Scripta **91**, 053002 (2016).

[48] H. Hergert, S. K. Bogner, T. D. Morris, A. Schwenk, and K. Tsukiyama, "The in-medium similarity renormalization group: A novel *ab initio* method for nuclei," Phys. Rept. **621**, 165 (2016).

[49] T. Papenbrock, "Effective theory for deformed nuclei," Nucl. Phys. A **852**, 36 (2011).

[50] J. Zhang and T. Papenbrock, "Rotational constants of multi-phonon bands in an effective theory for deformed nuclei," Phys. Rev. C **87**, 034323 (2013).

[51] T. Papenbrock and H. A. Weidenmüller, "Effective field theory for finite systems with spontaneously broken symmetry," Phys. Rev. C **89**, 014334 (2014).

[52] E. A. Coello Pérez and T. Papenbrock, "Effective theory for the nonrigid rotor in an electromagnetic field: Toward accurate and precise calculations of $E2$ transitions in deformed nuclei," Phys. Rev. C **92**, 014323 (2015).

[53] T. Papenbrock and H. A. Weidenmüller, "Effective field theory of emergent symmetry breaking in deformed atomic nuclei," J. Phys. G **42**, 105103 (2015).

[54] E. A. Coello Pérez and T. Papenbrock, "Effective field theory for nuclear vibrations with quantified uncertainties," Phys. Rev. C **92**, 064309 (2015).

[55] E. A. Coello Pérez and T. Papenbrock, "Effective field theory for vibrations in odd-mass nuclei," Phys. Rev. C **94**, 054316 (2016).

[56] A. P. Meshik, C. M. Hohenberg, O. V. Pravdivtseva, and Ya. S. Kapusta, "Weak decay of ^{130}Ba and ^{132}Ba: Geochemical measurements," Phys. Rev. C **64**, 035205 (2001).

[57] M. Pujol, B. Marty, P. Burnard, and P. Philippot, "Xenon in Archean barite: Weak decay of ^{130}Ba, mass-dependent isotopic fractionation and implication for barite formation," Geochim. Cosmochim. Acta **73**, 6834 (2009).

[58] Yu. M. Gavrilyuk, A. M. Gangapshev, V. V. Kazalov, V. V. Kuzminov, S. I. Panasenko, and S. S. Ratkevich, "Indications of $2\nu 2K$ capture in ^{78}Kr," Phys. Rev. C **87**, 035501 (2013).

[59] A. Bohr, "The coupling of nuclear surface oscillations to the motion of individual nucleons," Dan. Mat. Fys. Medd. **26**, 1 (1952).

[60] A. Bohr and B. R. Mottelson, "Collective and individual-particle aspects of nuclear structure," Dan. Mat. Fys. Medd. **27**, 1 (1953).

[61] A. Bohr and B. R. Mottelson, *Nuclear Structure*, Vol. II: Nuclear Deformations (W. A. Benjamin, New York, 1975).

[62] D. J. Rowe and J. L. Wood, *Fundamentals of Nuclear Models: Foundational Models*, 1st ed. (World Scientific Publishing Co. Pte. Ltd., Singapore, 2010).

[63] A. Arima and F. Iachello, "Collective Nuclear States as Representations of a SU(6) Group," Phys. Rev. Lett. **35**, 1069 (1975).

[64] A. Arima and F. Iachello, "Interacting boson model of collective states I. The vibrational limit," Ann. Phys. **99**, 253 (1976).

[65] A. Arima and F. Iachello, "Extension of the interacting boson model to odd-A nuclei," Phys. Rev. C **14**, 761 (1976).

[66] T. Otsuka, A. Arima, F. Iachello, and I. Talmi, "Shell model description of interacting bosons," Phys. Lett. B **76**, 139 (1978).

[67] T. Otsuka, A. Arima, and F. Iachello, "Nuclear shell model and interacting bosons," Nucl. Phys. A **309**, 1 (1978).

[68] F. Iachello and O. Scholten, "Interacting Boson-Fermion Model of Collective States in Odd-A Nuclei," Phys. Rev. Lett. **43**, 679 (1979).

[69] D. A. Varshalovich, A. N. Moskalev, and V. K. Khersonskii, *Quantum Theory of Angular Momentum*, 1st ed. (World Scientific Publishing Co. Pte. Ltd., Singapore, 1988).

[70] M. Sakai, "Hindrance phenomena in allowed beta transition from medium odd nuclei," Nucl. Phys. **33**, 96 (1962).

[71] A. L. Nichols, B. Singh, and J. K. Tuli, "Nuclear Data Sheets for A = 62," Nucl. Data Sheets **113**, 973 (2012).

[72] B. Singh, "Nuclear Data Sheets for A = 64," Nucl. Data Sheets **108**, 197 (2007).

[73] E. Browne and J. K. Tuli, "Nuclear Data Sheets for A

= 66," Nucl. Data Sheets **111**, 1093 (2010).
[74] E. A. McCutchan, "Nuclear Data Sheets for A = 68," Nucl. Data Sheets **113**, 1735 (2012).
[75] G. Gürdal and E. A. McCutchan, "Nuclear Data Sheets for A = 70," Nucl. Data Sheets **136**, 1 (2016).
[76] B. Singh, "Nuclear Data Sheets for A = 80," Nucl. Data Sheets **105**, 223 (2005).
[77] A. R. Farhan and B. Singh, "Nuclear Data Sheets for A = 78," Nucl. Data Sheets **110**, 1917 (2009).
[78] J. K. Tuli, "Nuclear Data Sheets for A = 82," Nucl. Data Sheets **98**, 209 (2003).
[79] B. Singh and Z. Hu, "Nuclear data sheets for A = 98," Nucl. Data Sheets **98**, 335 (2003).
[80] B. Singh, "Nuclear data sheets for A = 100," Nucl. Data Sheets **109**, 297 (2008).
[81] D. De Frenne, "Nuclear Data Sheets for A = 102," Nucl. Data Sheets **110**, 1745 (2009).
[82] J. Blachot, "Nuclear data sheets for A = 104," Nucl. Data Sheets **108**, 2035 (2007).
[83] D. De Frenne and A. Negret, "Nuclear Data Sheets for A = 106," Nucl. Data Sheets **109**, 943 (2008).
[84] J. Blachot, "Nuclear data sheets for A = 108," Nucl. Data Sheets **91**, 135 (2000).
[85] G. Gürdal and F. G. Kondev, "Nuclear Data Sheets for A = 110," Nucl. Data Sheets **113**, 1315 (2012).
[86] S. Lalkovski and F. G. Kondev, "Nuclear Data Sheets for A = 112," Nucl. Data Sheets **124**, 157 (2015).
[87] J. Blachot, "Nuclear data sheets for A = 114," Nucl. Data Sheets **113**, 515 (2012).
[88] J. Blachot, "Nuclear Data Sheets for A = 116," Nucl. Data Sheets **111**, 717 (2010).
[89] K. Kitao, "Nuclear Data Sheets Update for A = 118," Nucl. Data Sheets **75**, 99 (1995).
[90] K. Kitao, Y. Tendow, and A. Hashizume, "Nuclear Data Sheets for A = 120," Nucl. Data Sheets **96**, 241 (2002).
[91] T. Tamura, "Nuclear Data Sheets for A = 122," Nucl. Data Sheets **108**, 455 (2007).
[92] J. Katakura and Z. D. Wu, "Nuclear Data Sheets for A = 124," Nucl. Data Sheets **109**, 1655 (2008).
[93] Z. Elekes and J. Timar, "Nuclear Data Sheets for A = 128," Nucl. Data Sheets **129**, 191 (2015).
[94] B. Singh, "Nuclear Data Sheets for A = 130," Nucl. Data Sheets **93**, 33 (2001).
[95] J. W. Watson, W. Pairsuwan, B. D. Anderson, A. R. Baldwin, B. S. Flanders, R. Madey, R. J. McCarthy, B. A. Brown, B. H. Wildenthal, and C. C. Foster, "Relationship between Gamow-Teller transition probabilities and (p, n) cross sections at small momentum transfers," Phys. Rev. Lett. **55**, 1369 (1985).
[96] F. Molina, B. Rubio, Y. Fujita, W. Gelletly, J. Agramunt, A. Algora, J. Benlliure, P. Boutachkov, L. Cáceres, R. B. Cakirli, E. Casarejos, C. Domingo-Pardo, P. Doornenbal, A. Gadea, E. Ganioğlu, M. Gascón, H. Geissel, J. Gerl, M. Górska, J. Grębosz, R. Hoischen, R. Kumar, N. Kurz, I. Kojouharov, L. Amon Susam, H. Matsubara, A. I. Morales, Y. Oktem, D. Pauwels, D. Pérez-Loureiro, S. Pietri, Zs. Podolyák, W. Prokopowicz, D. Rudolph, H. Schaffner, S. J. Steer, J. L. Tain, A. Tamii, S. Tashenov, J. J. Valiente-Dobón, S. Verma, and H.-J. Wollersheim, "$T_z = -1 \to 0$ β decays of ^{54}Ni, ^{50}Fe, ^{46}Cr, and ^{42}Ti and comparison with mirror (^{3}He,t) measurements," Phys. Rev. C **91**, 014301 (2015).
[97] L. Popescu, T. Adachi, G. P. A. Berg, P. von Brentano, D. Frekers, D. De Frenne, K. Fujita, Y. Fujita, E.-W. Grewe, M. N. Harakeh, K. Hatanaka, E. Jacobs, K. Nakanishi, A. Negret, Y. Sakemi, Y. Shimbara, Y. Shimizu, Y. Tameshige, A. Tamii, M. Uchida, H. J. Wörtche, and M. Yosoi, "Gamow-teller transitions studied in the high-resolution ^{64}Ni(^{3}He, t)^{64}Cu reaction," Phys. Rev. C **79**, 064312 (2009).
[98] J. H. Thies, D. Frekers, T. Adachi, M. Dozono, H. Ejiri, H. Fujita, Y. Fujita, M. Fujiwara, E.-W. Grewe, K. Hatanaka, P. Heinrichs, D. Ishikawa, N. T. Khai, A. Lennarz, H. Matsubara, H. Okamura, Y. Y. Oo, P. Puppe, T. Ruhe, K. Suda, A. Tamii, H. P. Yoshida, and R. G. T. Zegers, "The (^{3}He,t) reaction on ^{76}Ge, and the double-β-decay matrix element," Phys. Rev. C **86**, 014304 (2012).
[99] D. Frekers, M. Alanssari, T. Adachi, B. T. Cleveland, M. Dozono, H. Ejiri, S. R. Elliott, H. Fujita, Y. Fujita, M. Fujiwara, K. Hatanaka, M. Holl, D. Ishikawa, H. Matsubara, H. Okamura, P. Puppe, K. Suda, A. Tamii, J. Thies, and H. P. Yoshida, "High energy-resolution measurement of the ^{82}Se(^{3}He, t)^{82}Br reaction for double-β decay and for solar neutrinos," Phys. Rev. C **94**, 014614 (2016).
[100] J. H. Thies, T. Adachi, M. Dozono, H. Ejiri, D. Frekers, H. Fujita, Y. Fujita, M. Fujiwara, E.-W. Grewe, K. Hatanaka, P. Heinrichs, D. Ishikawa, N. T. Khai, A. Lennarz, H. Matsubara, H. Okamura, Y. Y. Oo, P. Puppe, T. Ruhe, K. Suda, A. Tamii, H. P. Yoshida, and R. G. T. Zegers, "High-resolution ^{100}Mo(^{3}He,t)^{100}Tc charge-exchange experiment and the impact on double-β decays and neutrino charged-current reactions," Phys. Rev. C **86**, 044309 (2012).
[101] H. Akimune, H. Ejiri, M. Fujiwara, I. Daito, T. Inomata, R. Hazama, A. Tamii, H. Toyokawa, and M. Yosoi, "GT strengths studied by (^{3}He, t) reactions and nuclear matrix elements for double beta decays," Phys. Lett. B **394**, 23 (1997).
[102] P. Puppe, A. Lennarz, T. Adachi, H. Akimune, H. Ejiri, D. Frekers, H. Fujita, Y. Fujita, M. Fujiwara, E. Ganioğlu, E.-W. Grewe, K. Hatanaka, R. Hodak, C. Iwamoto, N. T. Khai, A. Okamoto, H. Okamura, P. P. Povinec, G. Susoy, T. Suzuki, A. Tamii, J. H. Thies, and M. Yosoi, "High resolution (^{3}He,t) experiment on the double-β decaying nuclei ^{128}Te and ^{130}Te," Phys. Rev. C **86**, 044603 (2012).
[103] Q. B. Chen, N. Kaiser, U.-G. Meißner, and J. Meng, "Effective field theory for triaxially deformed nuclei," Eur. Phys. J. A **53**, 204 (2017).
[104] J. Barea and F. Iachello, "Neutrinoless double-β decay in the microscopic interacting boson model," Phys. Rev. C **79**, 044301 (2009).